Targeting the Root Cause of Mucopolysaccharidosis IIIA with a New scAAV9 Gene Replacement Vector

Tierra A. Bobo,[1,2] Preston N. Samowitz,[1] Michael I. Robinson,[1] and Haiyan Fu[1,2]

[1]Gene Therapy Center, University of North Carolina at Chapel Hill, Chapel Hill, NC 27599, USA; [2]Division of Genetics and Metabolism, Department of Pediatrics, School of Medicine, University of North Carolina at Chapel Hill, Chapel Hill, NC 27599, USA

No treatment is available to address the unmet needs of mucopolysaccharidosis (MPS) IIIA patients. Targeting the root cause, we developed a new self-complementary adeno-associated virus 9 (scAAV9) vector to deliver the human *N*-sulfoglucosamine sulfohydrolase (hSGSH) gene driven by a miniature cytomegalovirus (mCMV) promoter. In pre-clinical studies, the vector was tested at varying doses by a single intravenous (i.v.) infusion into MPS IIIA mice at different ages. The vector treatments resulted in rapid and long-term expression of functional recombinant SGSH (rSGSH) enzyme and elimination of lysosomal storage pathology throughout the CNS and periphery in all tested animals. Importantly, MPS IIIA mice treated with the vector at up to 6 months of age showed significantly improved behavior performance in a hidden task in the Morris water maze, as well as extended lifespan, with most of the animals surviving within the normal range, indicating that the vector treatment can prevent and reverse MPS IIIA disease progression. Notably, 2.5×10^{12} vector genomes (vg)/kg was functionally effective. Furthermore, the vector treatment did not lead to detectable systemic toxicity or adverse events in MPS IIIA mice. These data demonstrate the development of a safe and effective new gene therapy product for treating MPS IIIA, which further support the extended clinical relevance of platform recombinant AAV9 (rAAV9 gene delivery for treating broad neurogenetic diseases.

INTRODUCTION

Mucopolysaccharidosis (MPS) IIIA is a devastating lysosomal storage disease (LSD) with severe neurolopathy. The disease is caused by autosomal recessive mutations in *N*-sulfoglucosamine sulfohydrolase (SGSH), a lysosomal enzyme that is essential for the degradation of a class of biologically important glycosaminoglycans (GAGs), heparan sulfate.[1,2] While the mutations are highly heterogeneous, the lack of functional SGSH results in lysosomal GAG storage in cells in virtually all organs, leading to multisystem manifestations with profound neuropathologies throughout the nervous system.[1,3] Infants with MPS IIIA appear normal at birth. Most MPS IIIA patients are diagnosed before the age of 6 years, when severe neurological disorders have developed. Premature death typically occurs in the second decade.[1,3,4] No treatment is currently available, and palliative care has been the only option for MPS IIIA. The blood-brain barrier (BBB) has been the major challenge to therapeutic development for neuropathic LSDs.

Gene therapy offers an ideal strategy for treating most LSDs by targeting the root cause, with the potential for long-term endogenous expression of functional recombinant enzymes by replacing the defective gene. Given the bystander effects of lysosomal enzymes, there is no need to transduce every cell to achieve the optimal therapeutic benefits. While numerous viral vectors have been studied targeting different LSDs, recombinant adeno-associated virus (rAAV) vectors have been the favored tools for gene delivery because of their safe profiles, long-term transgene expression, and diverse cell and tissue tropisms of different AAV serotypes.[5–8]

The mode of delivery remains the key to achieve maximal therapeutic impacts for MPS IIIA, given the global diffuse neuropathy and wide manifestations in all organs. The bystander cross-correction effects of SGSH allow functional benefits from a small number of transduced cells if well distributed within an organ. Numerous studies showed that direct brain gene delivery may not be feasible for treating MPS in humans,[9–13] although it is safe.[14–16] The greatest therapeutic benefits can be achieved by systemic gene delivery across the BBB, given the abundance of capillaries in the central nervous system (CNS). The demonstrated trans-BBB neurotropic AAV9 has offered an effective solution for CNS gene delivery,[17,18] leading to successes in developing gene therapy products for treating neurogenetic diseases, in animal models via systemic[19–27] or intrathecal delivery.[23,28–36] These studies have led to the investigational new drug (IND) approvals of systemic rAAV9 gene delivery clinical trials in patients with spinal muscular atrophy (SMA), MPS II, MPS IIIA, and MPS IIIB, and in intrathecal rAAV9 gene delivery clinical trials in patients with giant axonal neuropathy, MPS I, MPS II, and MPS IIIA. The demonstrated groundbreaking efficacy of intravenous (i.v.) AAV9 infusion in the SMA

Table 1. Study Design: Systemic scAAV9-mCMV-h*SGSH* Gene Delivery in MPS IIIA Mice

| Cohorts | Vector Dose (vg/kg) | Injection Age (m) | No. Mice (n) | | | | | | | |
| | | | Total | Behavior | | Necropsy | | | | |
				Age 8 Months	Age 12 Months	5 Days p.i.	1 Month p.i.	Age 8 Months	End	Longevity
1. MPS	2.5×10^{12}	1	18	12	–	–	5	5	5	8
2. MPS	5×10^{12}	1	22	18	–	–	4	5	9	13
3. MPS	1×10^{13}	3	9	5	5	–	4	–	5	5
4. MPS	1×10^{13}	6	6	6	5	–	–	–	6	6
5. MPS[a]	5×10^{13}	3–4	4	–	–	–	4	–		0
6. WT[a]	5×10^{13}	4	8	–	–	4	4	–	4	0
7. WT[a]	3×10^{13}	2	3	–	–	3	–	–	3	0
8. MPS[b]	–	–	63	36	–	–	5	5		53
9. WT[b]	–	–	75	75	6	–	5	5		53

–, not performed.
[a]Non-GLP toxicology testing.
[b]Controls combined from multiple experiments.

trial[37] led to the US Food and Drug Administration (FDA) approval of Zolgensma, further confirming the potential of systemic rAAV9 vector gene delivery as an effective platform tool for developing effective gene therapy targeting the root cause to treat neurogenetic diseases. Furthermore, studies using *ex vivo* gene therapy have also achieved successful correction of MPS IIIA neurological disease in mice.[38]

Taking advantage of both the high efficiency of the self-complementary AAV (scAAV) vector,[39–41] and AAV9 trans-BBB neurotropism in this study, we developed a new scAAV9-miniature cytomegalovirus (mCMV)-h*SGSH* vector, to address the still unmet need of MPS IIIA. We tested the vector in MPS IIIA mice at different disease stages to assess the clinical potential. A single i.v. scAAV9-human *SGSH* (h*SGSH*) delivery led to significant improvement in behavior and extension in survival within the range of normal lifespan in MPS IIIA mice, demonstrating the clinically meaningful benefits and the potential of this new scAAV9-h*SGSH* vector for treating the disease in humans via an i.v. injection.

RESULTS

In this study, we developed a new scAAV9 vector using a mCMV promoter to drive the expression of hSGSH. To determine the therapeutic potential of the scAAV9-mCMV-h*SGSH* gene therapy vector, we tested the vector in MPS IIIA mice at age 1, 3, or 6 months with an i.v. injection of the vector at 2.5×10^{12} vector genomes (vg)/kg (n = 18), 5×10^{12} vg/kg (n = 22), or 1×10^{13} vg/kg (cohorts 1–4). Behavior tests were conducted in all mice in a hidden task in a Morris water maze at 8 and/or 12 months of age (n = 6–18/group). Tissue analyses were performed for SGSH enzyme activity, GAG contents, histopathology, and biodistribution at 1 month postinjection (p.i.), 8 months of age (n = 4–5/group), or the humane endpoint. Subsets of mice from each group were observed for longevity (n = 6–13). To assess the potential acute toxicity, small groups of animals (cohorts 5–7) were

treated with the vector at higher doses, that is, 3×10^{13} or 5×10^{13} vg/kg. Controls were combined randomly and assigned to non-treated MPS IIIA and wild-type (WT) littermates. Table 1 summarizes the overall experimental design.

Significant Behavioral Improvement

To assess the functional neurological benefits of scAAV9-mCMV-h*SGSH* via i.v. delivery, the vector-treated mice were tested for performance in a hidden task in a Morris water maze at 8 months (Figures 1A and 1B) and/or 12 months of age (Figures 1B and 1C). The vector treatments led to significant improvement to WT levels in latency to find a hidden platform and swimming ability in MPS IIIA mice treated at 1 month of age with 2.5×10^{12} vg/kg (n = 12) or 5×10^{12} vg/kg (n = 18) when tested at 8 months of age, indicating the correction of cognitive and motor function. These data further support the notion of the functional dose threshold of an i.v. delivery of scAAV9-mCMV-h*SGSH*, because of the bystander effect of SGSH. MPS IIIA mice treated at age 3 months (n = 8) or 6 months (n = 6) with 1×10^{13} vg/kg vector showed normalized swimming ability, but only partial correction in latency to find the hidden platform when tested at age 8 months (Figures 1B and 1C). However, when re-tested at age 12 months, animals treated at age 3 months (n = 5) or 6 months (n = 5) showed latency and swimming ability similar to WT mice (n = 6) (Figures 1B and 1C). Notably, both WT and MPS IIIA mice treated with the vector at age 3 or 6 months showed further improvement in latency to find the hidden platform, rather than a decline in ability, when retested at age 12 months, compared to that of first test at age 8 months (Figures 1B and 1C). These data indicate that the vector treatment led to the correction of cognitive and motor function in MPS IIIA animals.
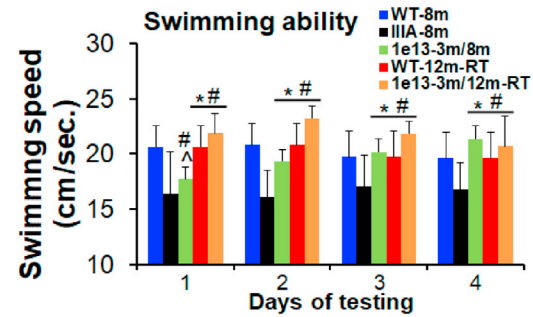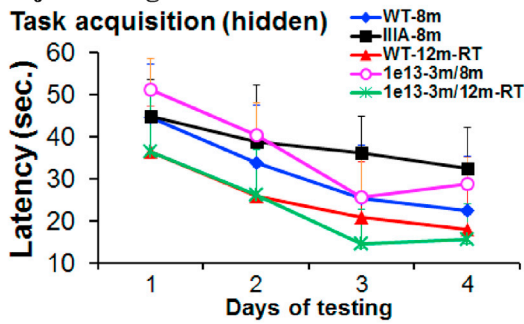
Significant Extension in Survival

Part of each cohort was maintained for longevity studies (Table 1). The results showed significantly increased survival in all MPS IIIA
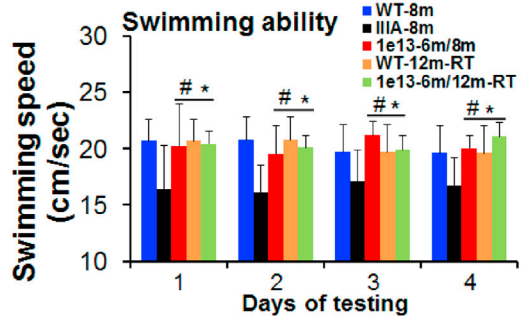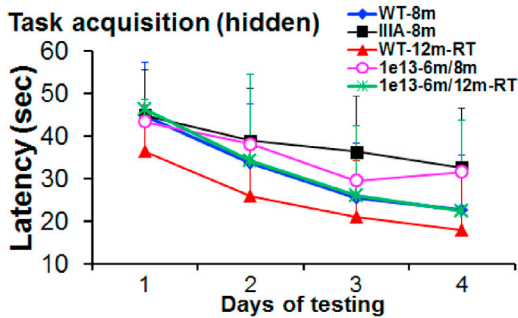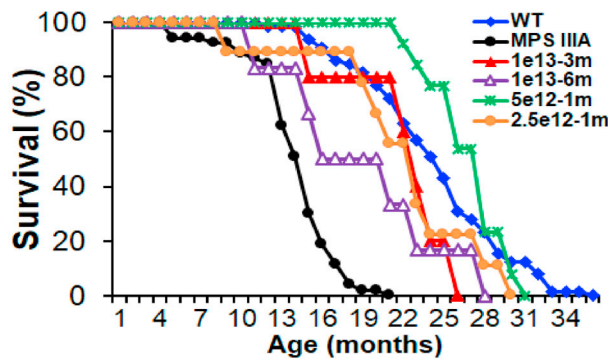
A Injection age: 1m
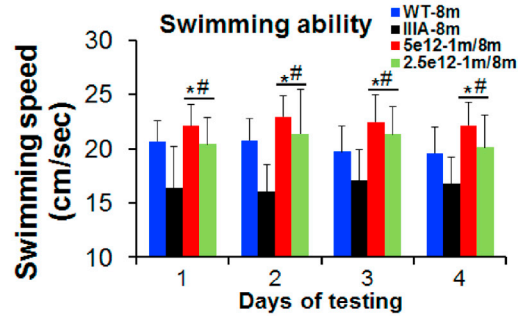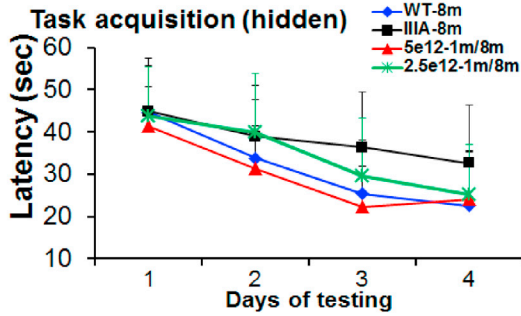
B Injection age: 3m

C Injection age: 6m

D Survival

(legend on next page)

mice that were treated with a i.v. delivery of the scAAV9-mCMV-h$SGSH$ vector. 90%–100% of MPS IIIA mice receiving 2.5×10^{12} or 5×10^{12} vg/kg vector at age 1 month, or 1×10^{13} vg/kg vector at age 3 month lived normal lifespans (Figure 1D). 80% of MPS mice treated with 1×10^{13} vg/kg vector at age 6 months also lived within the normal survival range (Figure 1D). Because neurological manifestation has been considered to be the cause of premature death in MPS IIIA, the significantly extended survival further supports the functional neurological impacts of the scAAV9-mCMV-h$SGSH$ vector via an i.v. infusion.

Rapid and Persistent Expression of Functional SGSH throughout the CNS and Periphery

To evaluate the persistence and levels of scAAV9-mediated rSGSH expression, tissues were assayed for SGSH activity at 1 month p.i., age 8 months, and the humane endpoint. The results showed SGSH activity at above normal levels in the liver, at close to normal levels in heart, spleen, and lung, and at subnormal levels in the brain, intestine, skeletal muscle, and kidney at 1 month p.i. in MPS IIIA mice treated with 2.5×10^{12}, 5×10^{12}, or 1×10^{13} vg/kg vector (Figures 2A–2C). Importantly, among all vector-treated MPS IIIA mice, brain SGSH activity was detected at 5.5%–18.2% of WT levels. Furthermore, SGSH activity levels persisted in the brain and most of the tested somatic tissues, while a significant decrease in SGSH activity was observed in the liver, spleen, and lung overtime from 1 month p.i. to the endpoint (Figures 2A–2C). Dose response was observed only in the liver and possibly in the spleen (Figures 2A and 2B). These results demonstrate that the scAAV9-mediated rSGSH expression is quick and persistent, and the rSGSH is enzymatically functional. The decrease in SGSH activity in liver, spleen, and lung over time may be due to the slow cell turnover and the predominantly episomal status of AAV vector.

Furthermore, tissues were also assayed for hSGSH by immunofluorescence (IF) staining to determine the distribution of the recombinant enzyme. The rSGSH expression was observed in cells throughout the CNS and peripheral tissues in vector-treated MPS IIIA mice (Figure 2D), correlating with the SGSH activity levels (Figures 2A–2C).

Lifelong Clearance of Lysosomal Storage Pathology and Correction of Astrocytosis

To further assess the functionality of scAAV9-mediated rSGSH, brain and multiple peripheral tissues were assayed for GAG contents at 1 month p.i., 8 months of age, or the humane endpoint. As shown in Figures 3A–3C, the vector treatments at all three tested doses led to significant reduction of GAG contents to normal levels in most of the tested tissues, including the brain and seven somatic tissues, with the exception of kidney. Importantly, the normalized tissue GAG contents were observed at all testing time points, from 1 month p.i. to the humane endpoint, in all MPS IIIA mice treated with the vector. These data further support that the scAAV9-mediated rSGSH is functional, leading to rapid clearance of GAG contents, as well as the correction and reversal of GAG storage in the CNS and periphery. Importantly, the complete clearance of tissue GAG storage persisted to the endpoint (Figures 3A–3C), correlating with the long-term tissue rSGSH expression (Figure 2). The clearance of lysosomal storage pathology was further confirmed by IF staining for lysosomal-associated membrane protein 1 (LAMP1), showing the reduction of LAMP1 in the brain and peripheral tissues (Figure 3D).

In addition, IF staining showed the clearance of glial fibrillary acidic protein (GFAP)-positive signals in the brain and retina (Figure 3D), indicating the correction of astrocytosis, a hallmark of neuroinflammation, in the CNS and optical nervous system (ONS). Unfortunately, we were not able to obtain data of IF LAMP1 and/or GFAP staining in intestine and other tissues, due to poor quality of tissue sections.

Differential Biodistribution of rAAV9-mCMV-hSGSH Vector Genome in the CNS and Periphery

To determine the biodistribution of scAAV9-mCMV-h$SGSH$ following an i.v. infusion, total tissue DNA samples were assayed using quantitative real-time PCR to quantitate scAAV9-h$SGSH$ vector genome in tissues at different time points after vector injection (n $\geq$ 4/group). We observed differential biodistribution of the vector DNA in tissues in MPS IIIA mice, with the highest vector genome levels detected in the liver, followed by heart, skeletal muscle, lung, intestine, kidney, spleen, and brain (Figure 4). Differences in tissue vector genome copy numbers were observed among MPS IIIA mice receiving scAAV9-mCMV-h$SGSH$ vector treatments. The vector genome copies persisted in most of the tissues, although decreases of vector genome were observed in liver, spleen, and lung over time.

Similar differential biodistribution profiles (Figure 5) were also observed in the small non-good laboratory practice (GLP) toxicology testing in MPS IIIA (cohort 5) and WT (cohorts 6 and 7) mice that received an i.v. injection of scAAV9-mCMV-h$SGSH$ at high doses (Table 1). The results showed a dose response of tissue vector genome in most of the tissues in WT mice at 1 month p.i. (Figure 5).

### No Observable Adverse Events and Detectable Toxicity

All mice used in this study were observed for potential adverse events following an i.v. injection of scAAV9-mCMV-h$SGSH$. No adverse events were seen in MPS IIIA mice treated with the vector at 2.5×10^{12}–1×10^{13} vg/kg in the efficacy studies during the entire experimental period until humane endpoints. Furthermore, no acute side

**Figure 1. Correction of Behavior Deficits and Extension in Survival**

MPS IIIA mice were treated with an i.v. injection of the scAAV9-mCMV-h$SGSH$ vector at 2.5×10^{12} or 5×10^{12} vg/kg at age 1 month, 1×10^{13} vg/kg at age 3 or 6 months. (A–C) Behavior performance was tested in a hidden task in a Morris water maze at age 8 months and/or 12 months. RT, mice treated at age 3 and 6 months were re-tested at age 12 m. WT and non-treated MPS IIIA mice were uses as controls. m/m, injection age/testing age (time). *p < 0.05 versus IIIA; ^p > 0.05 versus IIIA; #p > 0.05 versus WT. (D) Survival.
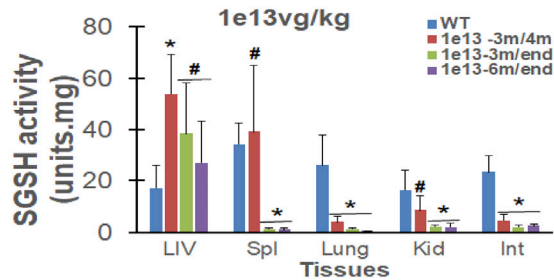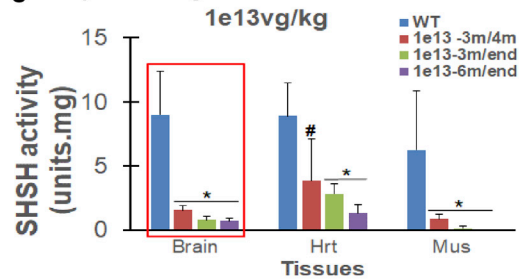
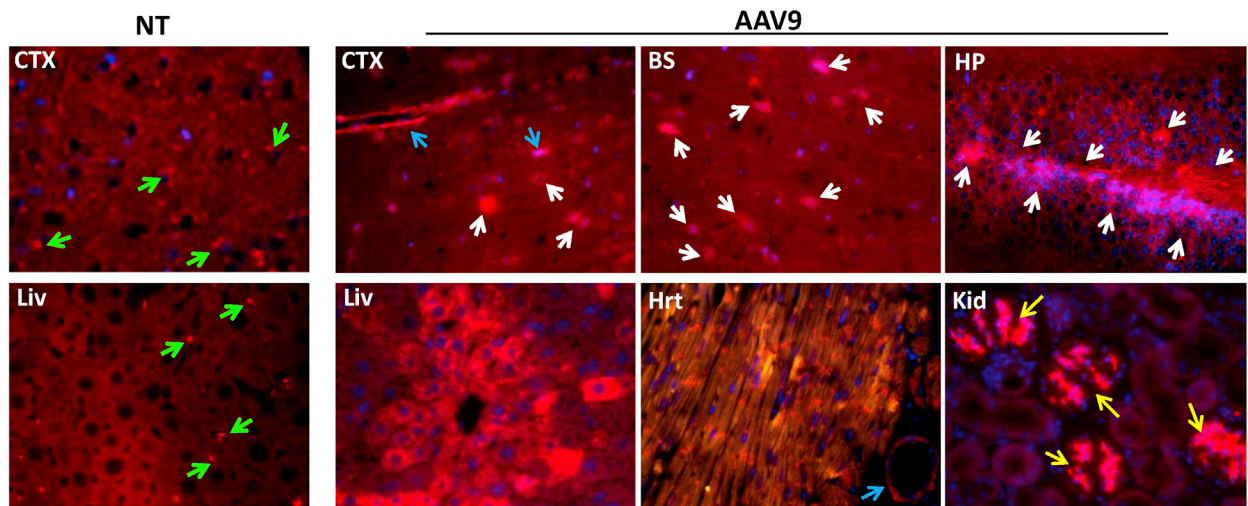**A** **Injection age: 1m**
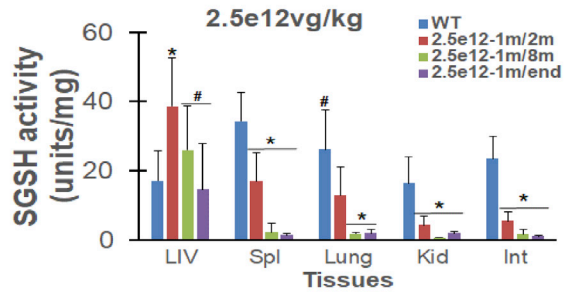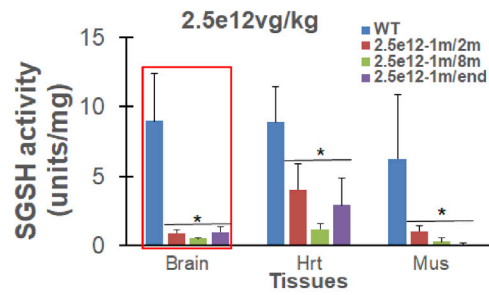
B **Injection age: 1m**
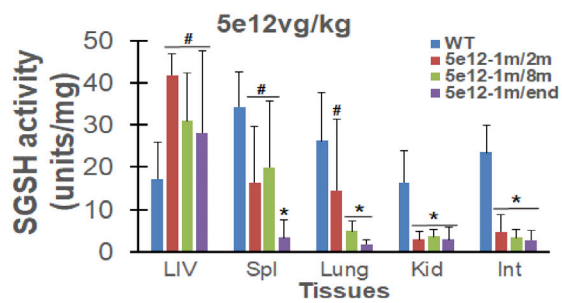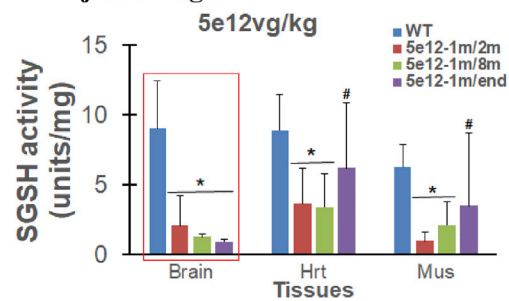
C **Injection age: 3m or 6m**

D 5×10^{12}vg/kg (injected at age 1m, assayed at 7m pi)

(legend on next page)

effects were observed in MPS IIIA and WT mice treated at a higher vector dose ($3x10^{13}$ or 5×10^{13} vg/kg) in short non-GLP toxicology studies. In addition, brain and seven somatic tissues from all mice in this study were processed for histopathology examination by a certified veterinary pathologist, and the results showed no detectable abnormality associated with the vector treatments in any animal subject. These data indicate that scAAV9-mCMV-h*SGSH* via an i.v. delivery were safe and did not induce systemic toxicity at tested doses.

DISCUSSION

In this study, we developed a new scAAV gene therapy vector using a truncated CMV promoter to drive h*SGSH* expression, targeting the root cause of MPS IIIA. We demonstrated the life-long functional benefits of scAAV9-mCMV-h*SGSH* via systemic delivery. A single i.v. infusion of the vector led to the effective restoration of SGSH enzyme activity before 1 month after vector treatment in an MPS IIIA mouse model. The expression of functional rSGSH persisted over the lifetime of the animals, resulting in the clearance of GAG storage in broad somatic tissues and throughout the CNS. The persistent therapeutic effects support the potential long-term beneficial impacts of this approach for treating MPS IIIA in humans.

We demonstrate in this preclinical study that at an effective dose, a single i.v. delivery of scAAV9-mCMV-h*SGSH*, is sufficient to not only prevent but also reverse the disease progression of MPS IIIA in mice. The reversibility has been a major concern in therapeutic development for MPS IIIA, since most of the patients are diagnosed after age 1–2 years, when severe neurological and somatic manifestations have already occurred. To address the reversibility issue, we tested the vector product in MPS IIIA mice at different ages (i.e., disease stages) and demonstrated that an i.v. infusion of scAAV9-mCMV-h*SGSH* at an effective dose can not only slow down, but also halt, the MPS IIIA disease progression. A single i.v. injection of 2.5×10^{12} and 5×10^{12} vg/kg scAAV9-mCMV-h*SGSH* in MPS IIIA mice at 1 month of age or 1×10^{13} vg/kg at age 3 or 6 months can mediate effective restoration of SGSH activity in all seven tested peripheral tissues and the brain. Importantly, the levels of rAAV9-mediated SGSH in tissues were sufficient to result in the life-long clearance of lysosomal GAG storage pathology, the correction of cognitive and motor functions, and mostly normalized survival. Notably, similar to findings in previous published studies,[27,42] our data further support the notion that a longer period of time is needed for the functional correction of neuropathological damage in mice treated at advanced disease stages. Interestingly, there was little clear correlation between tissue vector genome copies and rSGSH activity levels, suggesting differential transgene expression driven by the mCMV promoter. In all vector-treated MPS IIIA mice, tissue

(except kidney) GAG contents were reduced to levels comparable to those in WT mice through the study duration until the endpoints, indicating the effective clearance and reversal of lysosomal GAG accumulation in both the CNS and periphery, despite the variation in tissue rSGSH levels and the age of vector delivery. We therefore think that an i.v. infusion of scAAV9-mCMV-h*SGSH* at an effective dose can facilitate the expression of functional rSGSH at levels sufficient for the effective clearance of the CNS and somatic GAG storage, regardless of the disease stage to a certain extent, supporting its clinical potential for the treatment of MPS IIIA in patients.

Of the tested doses, the minimally efficacious dose (MED) of scAAV9-mCMV-h*SGSH* via a systemic delivery is 2.5×10^{12} vg/kg, which is 2-fold lower than the MED of the previous scAAV9-h*SGSH* vector product.[42] While a dose response was observed for rSGSH expression only in the liver and possibly spleen, complete clearance of GAG storage was achieved throughout the CNS and periphery, even at the lowest tested dose (2.5×10^{12} vg/kg) when treating MPS IIIA mice at age of 1 month. Notably, 4.5%–18.2% of WT levels of SGSH activity restored by an i.v. scAAV9-h*SGSH* infusion were sufficient to clear the lysosomal storage pathology and diminish the global neuropathology and neuroinflammation throughout the CNS, leading to the functional correction of neuropathy of MPS IIIA in all vector-treated mice. Strongly supported by previously published studies,[27,42,43] our data from this study reinforce the therapeutic potential of bystander effects of lysosomal enzymes, including SGSH, in gene therapy development targeting LSDs involving secretory lysosomal enzymes. The advantage of the bystander effects allows the achievement of optimal therapeutic benefits at significantly lower vector doses for treating LSDs, in comparison to rAAV gene therapy products for diseases involving a non-secreted protein, such as SMA (Zolgensma).[37,44] Therefore, the demonstrated lower MED of this new scAAV9-h*SGSH* vector product would ease the challenge in scale-up vector manufacture to the translation of this approach to clinical application to treat MPS IIIA in humans.

Furthermore, as expected, this study demonstrates the correction of MPS IIIA neuropathology beyond CNS in mice, following a single i.v. scAAV9-mCMV-h*SGSH* gene delivery. The vector treatment led to the amelioration of Müller glia activation and maintenance and restoration of the nuclear layers integrity in the retina, demonstrating the correction of gliosis and neurodegeneration in the ONS. Given that retinopathies are common in patients and mouse models with MPS III,[45–47] these are clinically meaningful observations that further support the extended clinical relevance of targeting the root cause by systemic scAAV9-h*SGSH* gene delivery for the treating MPS IIIA and other neurogenetic diseases.

Figure 2. Persistent Restoration of SGSH Activity in CNS and Somatic Tissues

(A–C) MPS IIIA mice were treated at age 1 month with an i.v. injection of 2.5×10^{12} vg/kg (A), 5×10^{12} vg/kg (B), or at 3 or 6 months with 1×10^{13} vg/kg (C) scAAV9-mCMV-h*SGSH* vector. (A–C) Tissues were assayed for SGSH activity at 1 month p.i. and age 8 months (n = 4–5/group) or the humane endpoint (n = 5–9). SGSH activity is expressed as U/mg protein; 1 U = nmol of 4MU released/17 h. *$p \leq 0.05$ versus WT; #$p > 0.05$ versus WT. (D) Tissues were assayed by immunofluorescence for hSGSH. Red fluorescence indicates rSGSH-positive signals; green arrows and yellow fluorescence indicates autofluorescence signals. NT, nontreated MPS IIIA mice; AAV9, AAV9-treated MPS IIIA mice. CTX, cerebral cortex; blue arrows indicate blood vessel; BS, brain stem; Liv, liver; Hrt, heart; green arrows indicate autofluorescent red blood cells; white arrows indicate hSGSH-positive brain cells; blue arrow indicates hSGSH-positive blood vessels; Kid, kidney; yellow arrows indicate glomerulus.

A 2.5e12vg/kg

B 5e12vg/kg

C 1e13vg/kg
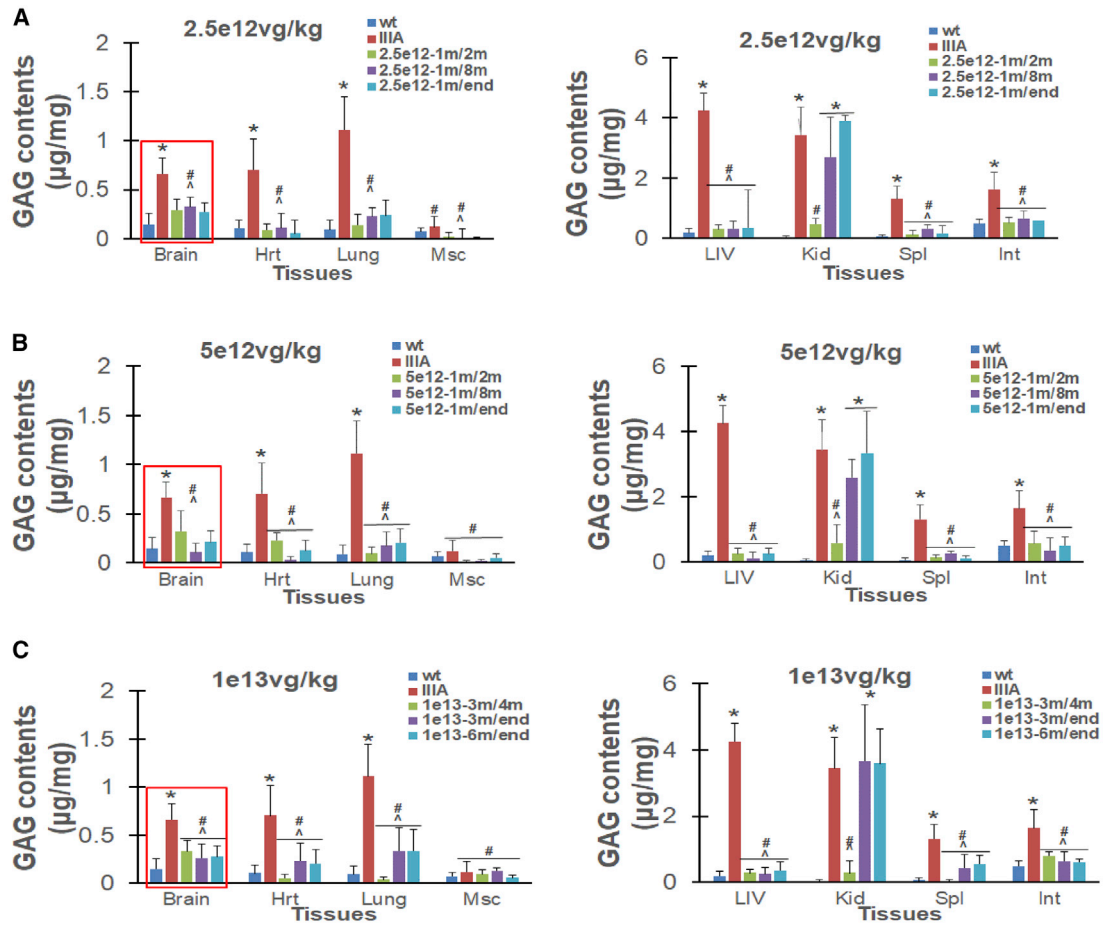
D Immunofluorescence (5x10^{12}vg/kg, injected at age 1m, assayed at 7m pi)

IF-LAMP1

IF-GFAP
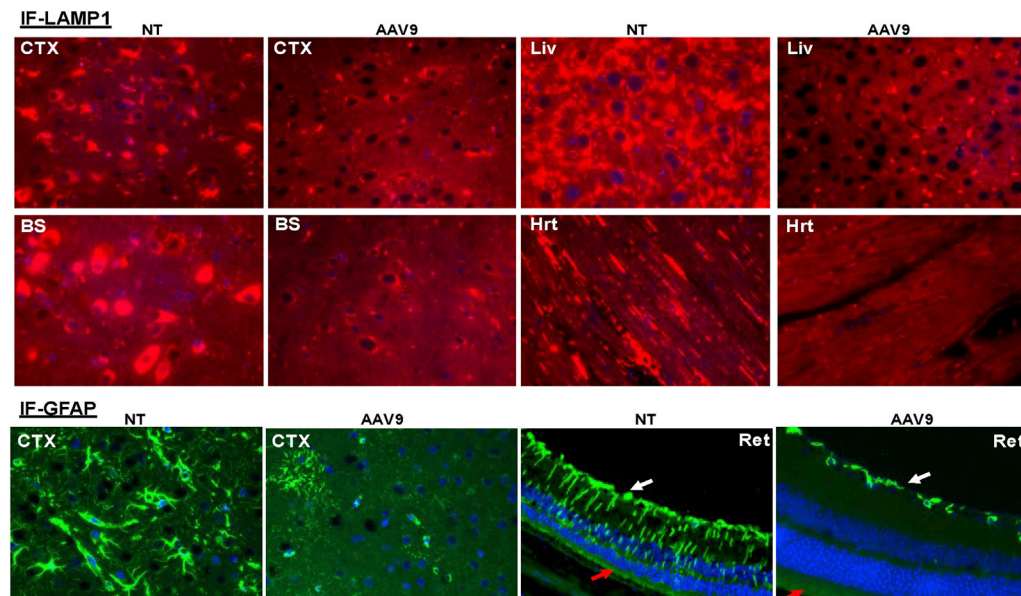
(legend on next page)

In summary, we developed a safe and potentially more effective new second-generation scAAV9-h*SGSH* gene therapy product for the treatment of MPS IIIA. This pre-clinical study demonstrates that systemic trans-BBB neurotropic AAV9 gene delivery targeting the root cause can prevent and reverse the broad neurological and somatic manifestations of the disease. In the present study, we demonstrate again that the efficacy and safety profiles of systemic rAAV9 gene delivery are highly reproducible, further supporting the potential of the demonstrated AAV9 vector platform for the effective translation of rAAV9 gene therapy products to clinical application to benefit broad neurogenetic disease patient populations.

MATERIALS AND METHODS

Animals
The MPS IIIA mice with spontaneous mutation (B6.Cg-*Sgsh*^{mps3a})[48] and their age-matched WT littermates were used in this study. The founder mice were kindly provided by Dr. S.U. Walkley (Albert Einstein College of Medicine). The MPS IIIA mouse colony has been maintained on an inbred background (C57BL/6) by backcrosses of heterozygotes in the animal facility in the University of North Carolina at Chapel Hill (UNC-CH). The progeny mice were genotyped by PCR with restriction digest.[48] The MPS IIIA mice retain approximately 3% residual SGSH activity, and they exhibit phenotypes resembling the human disease in virtually all aspects, including characteristic lysosomal storage pathology in cells of virtually all organs, progressive neurological disorders with relatively mild somatic manifestations, and a significantly shortened lifespan.

All animal care and procedures were performed strictly following the protocol approved by the Institutional Animal Care and Use Committee (IACUC) at UNC-CH, in accordance with the *Guide for the Care and Use of Laboratory Animals* (Eighth Edition, 2011).

Recombinant AAV Viral Vector
An scAAV vector plasmid (ptrs-mCMV-h*SGSH*) was constructed for the production of scAAV9-mCMV-h*SGSH* viral vector (Figure S1). The viral vector genome contains minimal elements essential for transgene expression, including AAV2 terminal repeats, a truncated 228-bp mCMV promoter,[27] human SGSH (h*SGSH*) coding sequence cDNA, and an SV40 polyadenylation signal (Figure S1). The viral vectors were produced at UNC Vector Core in HEK293 cells using three-plasmid co-transfection. The viral vector was purified by ion-exchange chromatography[49] and dialysis into 1× PBS (pH 7.0) containing 5% sorbitol and 350 mM NaCl. The titer of the vector was determined by quantitative real-time PCR using dot-blot titrated rAAV viral vector as the standard, and confirmed by dot-blot hybridization using the SGSH coding sequence as probe and serially diluted linearized ptrs-mCMV-h*SGSH* plasmid as the standard.

Systemic Vector Delivery
MPS IIIA mice were treated at different ages with an i.v. infusion of scAAV9-mCMV-h*SGSH* vector at different doses (in 150–200 μL of PBS) via the tail vein. For accuracy and consistency of vector delivery, mice were briefly anesthetized with isoflurane inhalation. Non-treated age- and sex-matched MPS IIIA and WT littermates were used as controls.

Behavioral Tests: Hidden Task in the Morris Water Maze
The scAAV9-mCMV-h*SGSH*-treated MPS IIIA mice and controls were tested for behavioral performance at approximately 8 months of age and/or age 12 months in a hidden task in a Morris water maze.[42,50] The water maze consisted of a large circular pool (diameter of 122 cm) filled with water (45 cm deep, 24°C–26°C) containing 1% white tempera paint, located in a room with numerous visual cues. Mice were tested for their ability to find a hidden escape platform (20 × 20 cm) 0.5 cm under the water surface. Each animal was given four trials per day, across 4 days. For each trial, the mouse was placed in the pool at one of four randomly ordered locations, and then given 60 s to swim to the hidden platform. If the mouse found the platform, the trial ended, and the animal was allowed to remain 10 s on the platform before the next trial began. If the platform was not found, the mouse was placed on the platform for 10 s, and then given the next trial. Measures were taken of latency to find the platform, swimming distance (cm), and swimming speed (cm/min) through an automated tracking system.

Longevity Observation
Following the scAAV9-mCMV-h*SGSH* vector injection, mice were continuously observed for the development of humane endpoint criteria, or until death occurred. The humane endpoint was when the symptoms of late stage MPS IIIA clinical manifestation (urine retention, rectal prolapse, protruding penis) became irreversible, or when mice showed significant weight loss, dehydration, or morbidity.

Tissue Analyses
Necropsies were performed at 1 month p.i., age 8 months, and/or the humane endpoint. Brain and multiple somatic tissues were harvested and stored at either −80°C or 4°C in 4% paraformaldehyde (in PBS, pH 7.2) prior to being processed for analyses.

SGSH Activity Assay
Tissue samples were assayed for SGSH enzyme activity following previously published procedures.[51] The assay measures 4-methylumbelliferone (4MU), a fluorescent product formed by two-step hydrolysis of the substrate 4-methylumbelliferyl-α-*N*-sulpho-D-glucosaminide. The sample SGSH activity desulfates the substrate during a 17-h reaction at 37°C, followed by a secondary reaction with excess α-glucosidase, releasing the fluorescent product 4MU during 24 h at 37°C. The SGSH activity is expressed as U/mg protein. One unit is equal to 1 nmol 4MU released/17 h.


Figure 3. Diminish of Lysosomal Storage Pathology and Astrocytosis

MPS IIIA mice were treated at age 1 month with an i.v. injection of the scAAV9-mCMV-h*SGSH* vector at different doses. (A–C) Tissues were assayed for GAG contents at 1 month p.i., age 8 months, or the humane endpoint. GAG content is expressed as μg/mg wet tissue. m/m indicates injection age/testing time. *p < 0.05 versus WT; #p > 0.05 versus WT; ^p ≤ 0.05 versus IIIA. (D) Immunofluorescence for LAMP1 (red fluorescence) or GFAP (green fluorescence). CTX, cerebral cortex; BS, brain stem; Liv, liver; Hrt, heart; Ret, retina; white arrows indicate inner surface; red arrows indicate choroid. NT indicates non-treated MPS IIIA; AAV9 indicates vector-treated MPS IIIA.

A   2.5x10¹²vg/kg: injection at age 1m
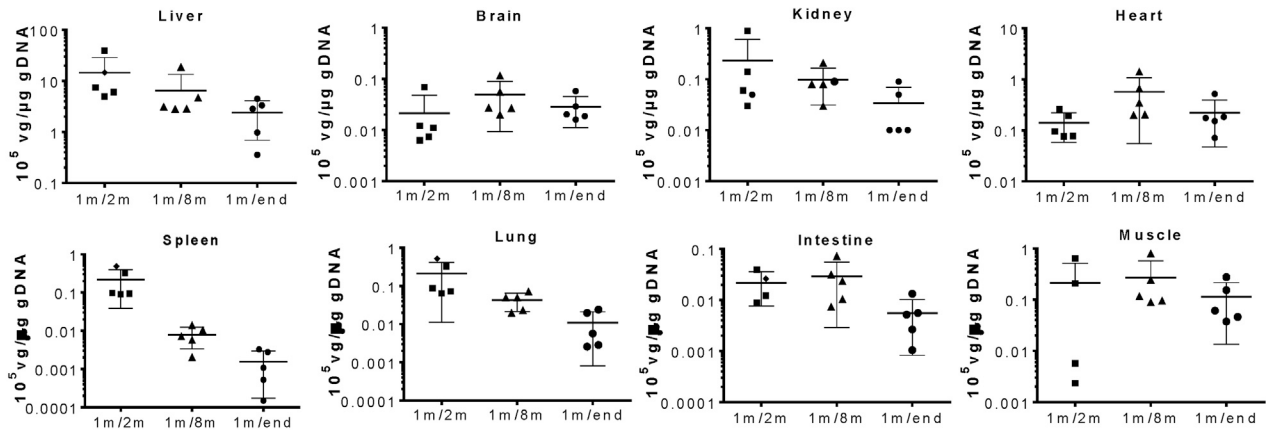
B   5x10¹²vg/kg: injection at age 1m
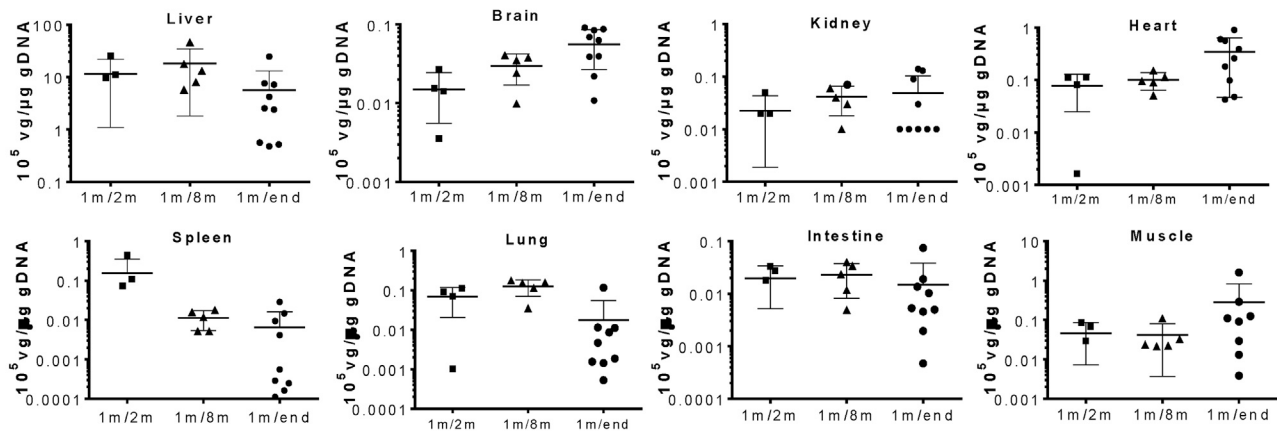
C   1x10¹³vg/kg: injection at age 3m, 6m
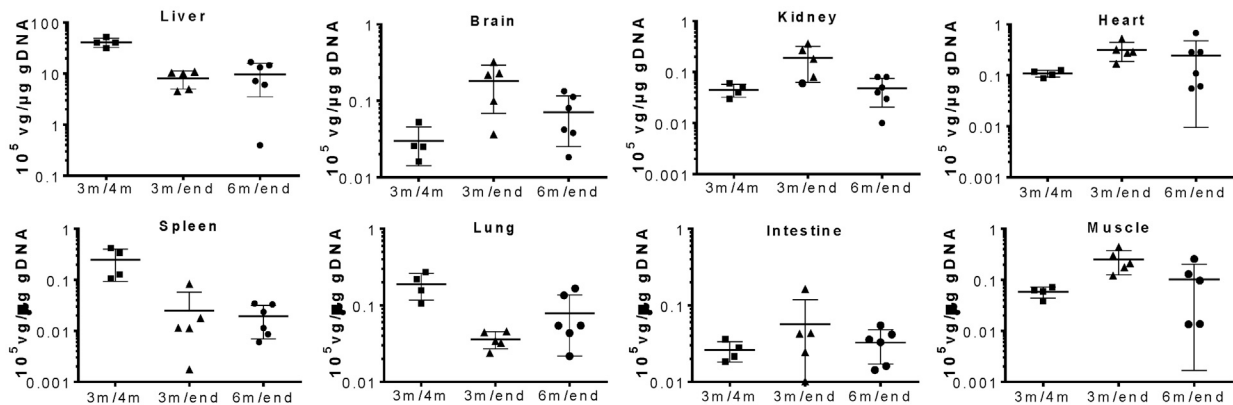
Figure 4. Biodistribution of Systemically Delivered scAAV9-mCMV-h*SGSH* in MPS IIIA Mice

(A–C) MPS IIIA mice were treated with an i.v. injection of scAAV9-mCMV-h*SGSH* at age 1 month at 2.5×10^{12} vg/kg (A), 5×10^{12} vg/kg (B), or 1×10^{13} vg/kg at age 3 or 6 months (C). Tissues were assayed in duplicates by quantitative real-time PCR at 1 month p.i., age 8 months, or the humane endpoint (n = 4–9/group). Data are expressed as 10^5 vector genomes (vg)/μg genomic DNA (gDNA). *Vector genome was detected at $<0.005 \times 10^5$ vg/μg gDNA in non-treated WT and MPS IIIA mice. m/m indicates injection age/testing time.
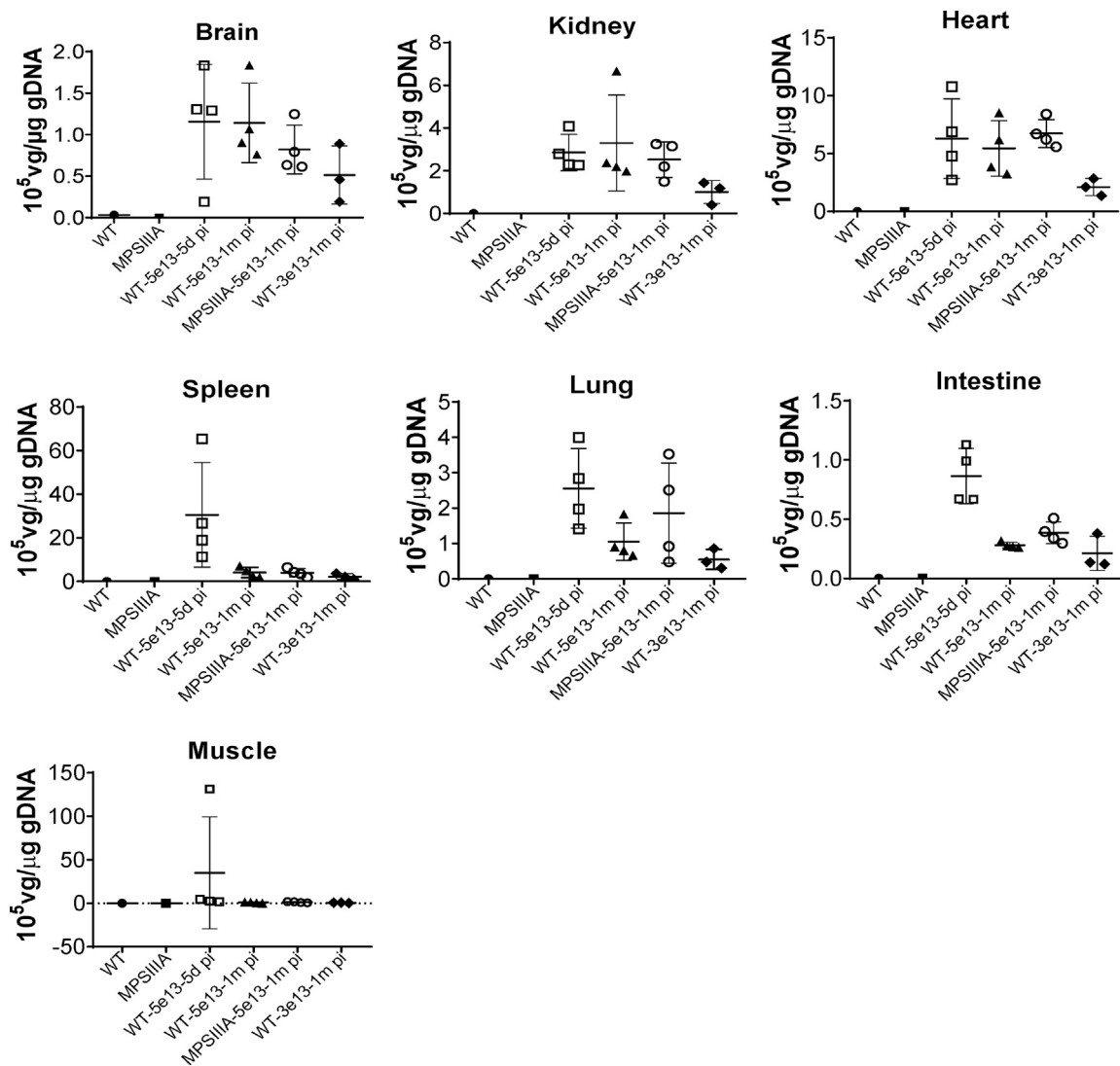
Figure 5. Differential Biodistribution of Systemically Delivered scAAV9-mCMV-h*SGSH* Vector in MPS IIIA and WT Mice

MPS IIIA and WT mice were treated at age 1–2 m with an i.v. injection of 3×10^{13} or 5×10^{13} vg/kg scAAV9-mCMV-h*SGSH*. Tissues were assayed by quantitative real-time PCR for the scAAV9-h*SGSH* vector genome at 5 days or 1 month p.i. (n = 3–4/group). Data are expressed as 10^5 vg/µg gDNA.

GAG Content Measurement

Tissues were processed to extract GAGs from published procedures with modifications.[52,53] A dimethylmethylene blue (DMB) assay was used to measure GAG content.[54] The GAG samples (from 0.5 to 1.0 mg tissue) were mixed with H_2O to 40 µL before adding 35 nM DMB (Polysciences, Warrington, PA, USA) in 0.2 mmol/L sodium formate buffer (pH 3.5). The product was measured using a spectrophotometer (optical density $[OD]_{535}$). The GAG content was expressed as µg/mg wet tissue.

IF Staining

Tissues were processed for thin paraffin sections (4 µm). IF staining was performed to identify cells expressing rSGSH, GFAP for astrocytes, or LAMP1 using antibodies against hSGSH (Abcam), GFAP (Millipore) or LAMP1 (Abcam), and corresponding secondary antibody conjugated with Alexa Fluor 568 or Alexa Fluor488 (Invitrogen), following procedures recommended by the manufacturers. The sections were visualized and imaged under a fluorescence microscope.

Quantitative Real-Time PCR

Total DNA was isolated from tissue samples using QIAGEN DNeasy columns. The DNA samples were assayed in duplicates by quantitative real-time PCR, using ABsolute Blue qPCR mix (Thermo Scientific) and an Applied Biosystems 7000 real-time PCR system, following the procedures recommended by the manufacturers. TaqMan primers specific for hSGSH were used to detect rAAV vector genomes as follows: forward, 5′-AAGTCAGCGAGGCCTACGT-3′; reverse,

5′-GATGGTCTTCGAGCCAAAGAT-3′; probe, 5′-(6-FAM)-CCTC CTAGACCTCACGCCCAC C-(TAMRA)-3′. Genomic DNA (gDNA) was quantified in parallel samples using mouse β-actin-specific primers as follows: forward, 5′-GTCATCACTAT TGGC AACGA-3′; reverse. 5′-CTCAGGA GTTTTGTCACCTT-3′, probe: 5′-(6-FAM)-TTCCGATG CCCTGAGGCTCT-(TAMRA)-3′. Serial diluted vector plasmid and mouse gDNA were used as standards. gDNA from tissues of non-treated mice were used as controls for background levels and absence of contamination. Data are expressed as vg/μg gDNA.

Histopathology
Brain and somatic tissues were processed to produce thin paraffin sections (4 μm) and then stained with hematoxylin and eosin (H&E). The H&E-stained tissue sections were examined by a board-certified veterinary pathologist at GEMpath (Longmont, CO, USA).

Statistical Analysis
Data were analyzed using Student's t test and/or a separate one-way ANOVAs to examine group differences. For all comparisons, significance was set at $p \leq 0.05$.

SUPPLEMENTAL INFORMATION
Supplemental Information can be found online at https://doi.org/10.1016/j.omtm.2020.10.014.

AUTHOR CONTRIBUTIONS
Conceptualization and Methodology, H.F. and T.A.B.; Investigation, T.A.B., P.N.S. and M.I.R.; Writing, T.A.B. and H.F.; Resources, Supervision, and Funding Acquisition, H.F.

DECLARATION OF INTERESTS
The authors declare no competing interests.

REFERENCES
1. Neufeld, E.F., and Muenzer, J. (2001). The mucopolysaccharidoses. In The Metabolic & Molecular Basis of Inherited Disease, Eighth Edition, C.R. Scriver, A.L. Beaudet, W.S. Sly, and D. Valle, eds. (McGraw-Hill), pp. 3421–3452.

2. Freeman, C., and Hopwood, J.J. (1986). Human liver sulphamate sulphohydrolase. Determinations of native protein and subunit M_r values and influence of substrate agylcone structure on catalytic properties. Biochem. J. 234, 83–92.

3. Yogalingam, G., and Hopwood, J.J. (2001). Molecular genetics of mucopolysaccharidosis type IIIA and IIIB: Diagnostic, clinical, and biological implications. Hum. Mutat. 18, 264–281.

4. Valstar, M.J., Ruijter, G.J., van Diggelen, O.P., Poorthuis, B.J., and Wijburg, F.A. (2008). Sanfilippo syndrome: a mini-review. J. Inherit. Metab. Dis. 31, 240–252.

5. Daya, S., and Berns, K.I. (2008). Gene therapy using adeno-associated virus vectors. Clin. Microbiol. Rev. 21, 583–593.

6. Zincarelli, C., Soltys, S., Rengo, G., and Rabinowitz, J.E. (2008). Analysis of AAV serotypes 1–9 mediated gene expression and tropism in mice after systemic injection. Mol. Ther. 16, 1073–1080.

7. Samulski, R.J., Chang, L.S., and Shenk, T. (1987). A recombinant plasmid from which an infectious adeno-associated virus genome can be excised in vitro and its use to study viral replication. J. Virol. 61, 3096–3101.

8. Berns, K.I., and Linden, R.M. (1995). The cryptic life style of adeno-associated virus. BioEssays 17, 237–245.

9. Desmaris, N., Verot, L., Puech, J.P., Caillaud, C., Vanier, M.T., and Heard, J.M. (2004). Prevention of neuropathology in the mouse model of Hurler syndrome. Ann. Neurol. 56, 68–76.

10. Fu, H., Samulski, R.J., McCown, T.J., Picornell, Y.J., Fletcher, D., and Muenzer, J. (2002). Neurological correction of lysosomal storage in a mucopolysaccharidosis IIIB mouse model by adeno-associated virus-mediated gene delivery. Mol. Ther. 5, 42–49.

11. Cressant, A., Desmaris, N., Verot, L., Bréjot, T., Froissart, R., Vanier, M.T., Maire, I., and Heard, J.M. (2004). Improved behavior and neuropathology in the mouse model of Sanfilippo type IIIB disease after adeno-associated virus-mediated gene transfer in the striatum. J. Neurosci. 24, 10229–10239.

12. Elliger, S.S., Elliger, C.A., Aguilar, C.P., Raju, N.R., and Watson, G.L. (1999). Elimination of lysosomal storage in brains of MPS VII mice treated by intrathecal administration of an adeno-associated virus vector. Gene Ther. 6, 1175–1178.

13. Passini, M.A., Watson, D.J., Vite, C.H., Landsburg, D.J., Feigenbaum, A.L., and Wolfe, J.H. (2003). Intraventricular brain injection of adeno-associated virus type 1 (AAV1) in neonatal mice results in complementary patterns of neuronal transduction to AAV2 and total long-term correction of storage lesions in the brains of β-glucuronidase-deficient mice. J. Virol. 77, 7034–7040.

14. McPhee, S.W., Janson, C.G., Li, C., Samulski, R.J., Camp, A.S., Francis, J., Shera, D., Lioutermann, L., Feely, M., Freese, A., and Leone, P. (2006). Immune responses to AAV in a phase I study for Canavan disease. J. Gene Med. 8, 577–588.

15. Hackett, N.R., Redmond, D.E., Sondhi, D., Giannaris, E.L., Vassallo, E., Stratton, J., Qiu, J., Kaminsky, S.M., Lesser, M.L., Fisch, G.S., et al. (2005). Safety of direct administration of $AAV2_{CU}hCLN2$, a candidate treatment for the central nervous system manifestations of late infantile neuronal ceroid lipofuscinosis, to the brain of rats and nonhuman primates. Hum. Gene Ther. 16, 1484–1503.

16. Tardieu, M., Zérah, M., Husson, B., de Bournonville, S., Deiva, K., Adamsbaum, C., Vincent, F., Hocquemiller, M., Broissand, C., Furlan, V., et al. (2014). Intracerebral administration of adeno-associated viral vector serotype rh.10 carrying human SGSH and SUMF1 cDNAs in children with mucopolysaccharidosis type IIIA disease: results of a phase I/II trial. Hum. Gene Ther. 25, 506–516.

17. Foust, K.D., Nurre, E., Montgomery, C.L., Hernandez, A., Chan, C.M., and Kaspar, B.K. (2009). Intravascular AAV9 preferentially targets neonatal neurons and adult astrocytes. Nat. Biotechnol. 27, 59–65.

18. Duque, S., Joussemet, B., Riviere, C., Marais, T., Dubreil, L., Douar, A.M., Fyfe, J., Moullier, P., Colle, M.A., and Barkats, M. (2009). Intravenous administration of self-complementary AAV9 enables transgene delivery to adult motor neurons. Mol. Ther. 17, 1187–1196.

19. Bevan, A.K., Duque, S., Foust, K.D., Morales, P.R., Braun, L., Schmelzer, L., Chan, C.M., McCrate, M., Chicoine, L.G., Coley, B.D., et al. (2011). Systemic gene delivery in large species for targeting spinal cord, brain, and peripheral tissues for pediatric disorders. Mol. Ther. 19, 1971–1980.

20. Fu, H., Dirosario, J., Killedar, S., Zaraspe, K., and McCarty, D.M. (2011). Correction of neurological disease of mucopolysaccharidosis IIIB in adult mice by rAAV9 trans-blood-brain barrier gene delivery. Mol. Ther. 19, 1025–1033.

21. Ruzo, A., Marcó, S., García, M., Villacampa, P., Ribera, A., Ayuso, E., Maggioni, L., Mingozzi, F., Haurigot, V., and Bosch, F. (2012). Correction of pathological accumulation of glycosaminoglycans in central nervous system and peripheral tissues of MPSIIIA mice through systemic AAV9 gene transfer. Hum. Gene Ther. 23, 1237–1246.

22. Weismann, C.M., Ferreira, J., Keeler, A.M., Su, Q., Qui, L., Shaffer, S.A., Xu, Z., Gao, G., and Sena-Esteves, M. (2015). Systemic AAV9 gene transfer in adult GM1 ganglio-sidosis mice reduces lysosomal storage in CNS and extends lifespan. Hum. Mol. Genet. 24, 4353–4364.

23. Gurda, B.L., De Guilhem De Lataillade, A., Bell, P., Zhu, Y., Yu, H., Wang, P., Bagel, J., Vite, C.H., Sikora, T., Hinderer, C., et al. (2016). Evaluation of AAV-mediated gene therapy for central nervous system disease in canine mucopolysaccharidosis VII. Mol. Ther. 24, 206–216.

24. Lee, N.C., Muramatsu, S., Chien, Y.H., Liu, W.S., Wang, W.H., Cheng, C.H., Hu, M.K., Chen, P.W., Tzen, K.Y., Byrne, B.J., and Hwu, W.L. (2015). Benefits of neuronal preferential systemic gene therapy for neurotransmitter deficiency. Mol. Ther. 23, 1572–1581.

25. Murrey, D.A., Naughton, B.J., Duncan, F.J., Meadows, A.S., Ware, T.A., Campbell, K.J., Bremer, W.G., Walker, C.M., Goodchild, L., Bolon, B., et al. (2014). Feasibility and safety of systemic rAAV9-hNAGLU delivery for treating mucopolysaccharidosis IIIB: toxicology, biodistribution, and immunological assessments in primates. Hum. Gene Ther. Clin. Dev. 25, 72–84.

26. Meadows, A.S., Duncan, F.J., Camboni, M., Waligura, K., Montgomery, C., Zaraspe, K., Naughton, B.J., Bremer, W.G., Shilling, C., Walker, C.M., et al. (2015). A GLP-compliant toxicology and biodistribution study: systemic delivery of an rAAV9 vec-tor for the treatment of mucopolysaccharidosis IIIB. Hum. Gene Ther. Clin. Dev. 26, 228–242.

27. Fu, H., Zaraspe, K., Murakami, N., Meadows, A.S., Pineda, R.J., McCarty, D.M., and Muenzer, J. (2018). Targeting root cause by systemic scAAV9-hIDS gene delivery: functional correction and reversal of severe MPS II in mice. Mol. Ther. Methods Clin. Dev. 10, 327–340.

28. Haurigot, V., and Bosch, F. (2013). Toward a gene therapy for neurological and so-matic MPSIIIA. Rare Dis. 1, e27209.

29. Hinderer, C., Bell, P., Gurda, B.L., Wang, Q., Louboutin, J.P., Zhu, Y., Bagel, J., O'Donnell, P., Sikora, T., Ruane, T., et al. (2014). Intrathecal gene therapy corrects CNS pathology in a feline model of mucopolysaccharidosis I. Mol. Ther. 22, 2018–2027.

30. Ribera, A., Haurigot, V., Garcia, M., Marcó, S., Motas, S., Villacampa, P., Maggioni, L., León, X., Molas, M., Sánchez, V., et al. (2015). Biochemical, histological and func-tional correction of mucopolysaccharidosis type IIIB by intra-cerebrospinal fluid gene therapy. Hum. Mol. Genet. 24, 2078–2095.

31. Duque, S.I., Arnold, W.D., Odermatt, P., Li, X., Porensky, P.N., Schmelzer, L., Meyer, K., Kolb, S.J., Schümperli, D., Kaspar, B.K., and Burghes, A.H. (2015). A large animal model of spinal muscular atrophy and correction of phenotype. Ann. Neurol. 77, 399–414.

32. Meyer, K., Ferraiuolo, L., Schmelzer, L., Braun, L., McGovern, V., Likhite, S., Michels, O., Govoni, A., Fitzgerald, J., Morales, P., et al. (2015). Improving single injection CSF delivery of AAV9-mediated gene therapy for SMA: a dose-response study in mice and nonhuman primates. Mol. Ther. 23, 477–487.

33. Mussche, S., Devreese, B., Nagabhushan Kalburgi, S., Bachaboina, L., Fox, J.C., Shih, H.J., Van Coster, R., Samulski, R.J., and Gray, S.J. (2013). Restoration of cytoskeleton homeostasis after gigaxonin gene transfer for giant axonal neuropathy. Hum. Gene Ther. 24, 209–219.

34. Hinderer, C., Katz, N., Louboutin, J.P., Bell, P., Yu, H., Nayal, M., Kozarsky, K., O'Brien, W.T., Goode, T., and Wilson, J.M. (2016). Delivery of an adeno-associated virus vector into cerebrospinal fluid attenuates central nervous system disease in mu-copolysaccharidosis type II mice. Hum. Gene Ther. 27, 906–915.

35. Motas, S., Haurigot, V., Garcia, M., Marcó, S., Ribera, A., Roca, C., Sánchez, X., Sánchez, V., Molas, M., Bertolin, J., et al. (2016). CNS-directed gene therapy for the treatment of neurologic and somatic mucopolysaccharidosis type II (Hunter syn-drome). JCI Insight 1, e86696.

36. Osborn, M.J., McElmurry, R.T., Peacock, B., Tolar, J., and Blazar, B.R. (2008). Targeting of the CNS in MPS-IH using a nonviral transferrin-a-l-iduronidase fusion gene product. Mol. Ther. 16, 1459–1466.

37. Mendell, J.R., Al-Zaidy, S., Shell, R., Arnold, W.D., Rodino-Klapac, L.R., Prior, T.W., Lowes, L., Alfano, L., Berry, K., Church, K., et al. (2017). Single-dose gene-replace-ment therapy for spinal muscular atrophy. N. Engl. J. Med. 377, 1713–1722.

38. Sergijenko, A., Langford-Smith, A., Liao, A.Y., Pickford, C.E., McDermott, J., Nowinski, G., Langford-Smith, K.J., Merry, C.L., Jones, S.A., Wraith, J.E., et al. (2013). Myeloid/microglial driven autologous hematopoietic stem cell gene therapy corrects a neuronopathic lysosomal disease. Mol. Ther. 21, 1938–1949.

39. Scott, H.S., Blanch, L., Guo, X.H., Freeman, C., Orsborn, A., Baker, E., Sutherland, G.R., Morris, C.P., and Hopwood, J.J. (1995). Cloning of the sulphamidase gene and identification of mutations in Sanfilippo A syndrome. Nat. Genet. 11, 465–467.

40. McCarty, D.M., Fu, H., Monahan, P.E., Toulson, C.E., Naik, P., and Samulski, R.J. (2003). Adeno-associated virus terminal repeat (TR) mutant generates self-comple-mentary vectors to overcome the rate-limiting step to transduction in vivo. Gene Ther. 10, 2112–2118.

41. McCarty, D.M., Monahan, P.E., and Samulski, R.J. (2001). Self-complementary re-combinant adeno-associated virus (scAAV) vectors promote efficient transduction independently of DNA synthesis. Gene Ther. 8, 1248–1254.

42. Fu, H., Cataldi, M.P., Ware, T.A., Zaraspe, K., Meadows, A.S., Murrey, D.A., and McCarty, D.M. (2016). Functional correction of neurological and somatic disorders at later stages of disease in MPS IIIA mice by systemic scAAV9-hSGSH gene delivery. Mol. Ther. Methods Clin. Dev. 3, 16036.

43. DiRosario, J., Divers, E., Wang, C., Etter, J., Charrier, A., Jukkola, P., Auer, H., Best, V., Newsom, D.L., McCarty, D.M., and Fu, H. (2009). Innate and adaptive immune activation in the brain of MPS IIIB mouse model. J. Neurosci. Res. 87, 978–990.

44. Foust, K.D., Wang, X., McGovern, V.L., Braun, L., Bevan, A.K., Haidet, A.M., Le, T.T., Morales, P.R., Rich, M.M., Burghes, A.H., et al. (2010). Rescue of the spinal muscular atrophy phenotype in a mouse model by early postnatal delivery of SMN. Nat. Biotechnol. 28, 271–274.

45. Ashworth, J.L., Biswas, S., Wraith, E., and Lloyd, I.C. (2006). Mucopolysaccharidoses and the eye. Surv. Ophthalmol. 51, 1–17.

46. Heldermon, C.D., Hennig, A.K., Ohlemiller, K.K., Ogilvie, J.M., Herzog, E.D., Breidenbach, A., Vogler, C., Wozniak, D.F., and Sands, M.S. (2007). Development of sensory, motor and behavioral deficits in the murine model of Sanfilippo syndrome type B. PLoS ONE 2, e772.

47. Summers, C.G., and Ashworth, J.L. (2011). Ocular manifestations as key features for diagnosing mucopolysaccharidoses. Rheumatology (Oxford) 50 (Suppl 5), v34–v40.

48. Bhaumik, M., Muller, V.J., Rozaklis, T., Johnson, L., Dobrenis, K., Bhattacharyya, R., Wurzelmann, S., Finamore, P., Hopwood, J.J., Walkley, S.U., et al. (1999). A mouse model for mucopolysaccharidosis type III A (Sanfilippo syndrome). Glycobiology 9, 1389–1396.

49. Grieger, J.C., Soltys, S.M., and Samulski, R.J. (2016). Production of recombinant ad-eno-associated virus vectors using suspension HEK293 cells and continuous harvest of vector from the culture media for GMP FIX and FLT1 clinical vector. Mol. Ther. 24, 287–297.

50. Warburton, E.C., Baird, A., Morgan, A., Muir, J.L., and Aggleton, J.P. (2001). The conjoint importance of the hippocampus and anterior thalamic nuclei for allocentric spatial learning: evidence from a disconnection study in the rat. J. Neurosci. 21, 7323–7330.

51. Karpova, E.A., Voznyi YaV, Keulemans, J.L., Hoogeveen, A.T., Winchester, B., Tsvetkova, I.V., and van Diggelen, O.P. (1996). A fluorimetric enzyme assay for the diagnosis of Sanfilippo disease type A (MPS IIIA). J. Inherit. Metab. Dis. 19, 278–285.

52. van de Lest, C.H., Versteeg, E.M., Veerkamp, J.H., and van Kuppevelt, T.H. (1994). Quantification and characterization of glycosaminoglycans at the nanogram level by a combined azure A-silver staining in agarose gels. Anal. Biochem. 221, 356–361.

53. Fu, H., Kang, L., Jennings, J.S., Moy, S.S., Perez, A., Dirosario, J., McCarty, D.M., and Muenzer, J. (2007). Significantly increased lifespan and improved behavioral perfor-mances by rAAV gene delivery in adult mucopolysaccharidosis IIIB mice. Gene Ther. 14, 1065–1077.

54. de Jong, J.G., Wevers, R.A., Laarakkers, C., and Poorthuis, B.J. (1989). Dimethylmethylene blue-based spectrophotometry of glycosaminoglycans in un-treated urine: a rapid screening procedure for mucopolysaccharidoses. Clin. Chem. 35, 1472–1477.